EBioMedicine xxx (xxxx) xxx

Contents lists available at ScienceDirect

EBioMedicine

journal homepage: www.ebiomedicine.com

EBioMedicine
Published by THE LANCET

Research Paper

Mapping of γ/δ T cells reveals Vδ2+ T cells resistance to senescence

Weili Xu [a,b], Gianni Monaco [a,c], Eleanor Huijin Wong [d], Wilson Lek Wen Tan [d], Hassen Kared [a], Yannick Simoni [a], Shu Wen Tan [a,e], Wilson Zhi Yong How [a], Crystal Tze Ying Tan [a], Bernett Teck Kwong Lee [a], Daniel Carbajo [a], Srinivasan K.G. [a], Ivy Chay Huang Low [a], Esther Wing Hei Mok [a], Shihui Foo [a], Josephine Lum [a], Hong Liang Tey [f], Wee Ping Tan [f], Michael Poidinger [a], Evan Newell [a], Tze Pin Ng [g], Roger Foo [d], Arne N. Akbar [h], Tamas Fülöp [i], Anis Larbi [a,b,j,k,*]

[a] Singapore Immunology Network (SIgN), Agency for Science Technology and Research (A*STAR), Immunos Building, Singapore 138648, Singapore
[b] School of Biological Sciences, Nanyang Technological University, Singapore, Singapore
[c] Department of Biomedicine, University Hospital Basel, Basel, Switzerland
[d] Genome Institute of Singapore (GIS), Agency for Science Technology and Research (A*STAR), Genome Building, Biopolis, Singapore, Singapore
[e] Immunology Programme, Department of Microbiology and Immunology, Yong Loo Lin School of Medicine, Life Sciences Institute, National University of Singapore, Singapore, Singapore
[f] National Skin Center, Singapore, Singapore
[g] Gerontology Research Programme, Department of Psychological Medicine, National University Health System, Yong Loo Lin School of Medicine, National University of Singapore, Singapore, Singapore
[h] Institute of Immunity and Transplantation, University College London, London, United Kingdom
[i] Research Center on Aging, Graduate Program in Immunology, Faculty of Medicine and Health Sciences, University of Sherbrooke, Sherbrooke, Quebec, Canada
[j] Department of Microbiology, National University of Singapore, Singapore, Singapore
[k] Department of Biology, Faculty of Science, University Tunis El Manar, Tunis, Tunisia

ARTICLE INFO

Article history:
Received 14 October 2018
Received in revised form 20 November 2018
Accepted 27 November 2018
Available online xxxx

Keywords:
Gamma Delta T cells
Immunosenescence
Innate Immunity
Immunobiology
Aging
Cellular Senescence

ABSTRACT

Background: Immune adaptation with aging is a major of health outcomes. Studies in humans have mainly focus on αβ T cells while γδ T cells have been neglected despite their role in immunosurveillance. We investigated the impact of aging on γδ T cell subsets phenotypes, functions, senescence and their molecular response to stress.
Methods: Peripheral blood of young and old donors in Singapore have been used to assess the phenotype, functional capacity, proliferation capacity and gene expression of the various γδ T cell subsets. Peripheral blood mononuclear cells from apheresis cones and young donors have been used to characterize the telomere length, epigenetics profile and DNA damage response of the various γδ T cell subsets phenotype.
Findings: Our data shows that peripheral Vδ2+ phenotype, functional capacity (cytokines, cytotoxicity, proliferation) and gene expression profile are specific when compared against all other αβ and γδ T cells in aging. Hallmarks of senescence including telomere length, epigenetic profile and DNA damage response of Vδ2+ also differs against all other αβ and γδ T cells.
Interpretation: Our results highlight the differential impact of lifelong stress on γδ T cells subsets, and highlight possible mechanisms that enable Vδ2+ to be resistant to cellular aging. The new findings reinforce the concept that Vδ2+ have an "innate-like" behavior and are more resilient to the environment as compared to "adaptive-like" Vδ1+ T cells.

1. Introduction

Aging has been associated with higher susceptibility to infections, cancer and also reduced vaccination efficacy [1,2]. This phenomenon could be due to a change in functionality of the immune system with age, otherwise known as immunosenescence [3]. Most of the studies in this field have focused on αβ T cells whereas γδ T cells have been neglected despite their important role against foreign pathogens and immunosurveillance [4,5].

γδ T cells are classified in between the adaptive and the innate immune system as they exhibit faster immune response to new infections compared to αβ T cells [6]. While αβ T cells react to major histocompatibility complex (MHC)-Class bound peptides, γδ T cells recognize a range of molecules and are not entirely MHC-Class dependent [7,8]. For instance, Vδ1+ react against stress-induced molecules such as MICA, MICB and ULBPs on infected or transformed cells [9,10]. Vδ2+

* Corresponding author at: Singapore Immunology Network (SIgN), Agency for Science Technology and Research (A*STAR), Immunos Building, Singapore 138648, Singapore
E-mail address: anis_larbi@immunol.a-star.edu.sg (A. Larbi).

https://doi.org/10.1016/j.ebiom.2018.11.053

Research in context

Evidence before the study

Evidences prior to this study suggests that γδ T cells in human peripheral blood do not seem to exhibit the same phenomenon of cellular differentiation/senescence with life-long stressors (i.e. CMV & Aging) as the classical αβ CD4 and CD8 T cells.

Added value of this study

Analyzing the individual γδ T cells subsets separately, we uncovered differences in the way life-long stresses (i.e. CMV and Aging) impacts on the different subsets of γδ T cells, the functionally relevant surface markers for the γδ T cells subsets and also possible pathways that enable Vδ2 + T cells to be resistant to cellular senescence.

Implication of all the available evidence

This offers new perspective on how we should analyze and classify human γδ T cells for future studies, the differential impact of life-long stresses on the different human γδ T cells subsets and the functionally-relevant surface markers for the different human γδ T cells subsets. Investigating the other mechanisms that Vδ2+ T cells utilizes to resist cellular senescence with age could also allow scientists to modulate or enhance T cell immunity of the elderly in the future, which will lead to better health-span and quality of life in old age.

respond against phospho-antigens (such as isopentenyl pyrophosphate (IPP) of the mevalonate pathway) that are elevated in tumor cells [11] and (E)-4-Hydroxy-3-methyl-but-2-enyl pyrophosphate (HMBPP) that is produced by bacteria and parasites [12].

Often in human studies of immunosenescence, accompanying infections such as Cytomegalovirus (CMV) have to be taken into account, as they are known to drive αβ T cell differentiation, which eventually leads αβ T cells into replicative senescence stage [13]. To study αβ T cells and their subsets, phenotypic markers such as CD27, CD45RA and CD57 are widely used as they functionally define the different subsets [14,15]. However, it is still controversial whether these markers have the same functional relevance for γδ T cells. Thus, our aim in the present study was to investigate the impact of aging and CMV on γδ T cell subsets phenotypes, functions, senescence and their molecular response to stress.

In the present study, using CMV history and aging as a model, we discovered that Vδ2+ T cells do not adhere closely to the phenotypes that have been defined for αβ T cells and are more resilient to cellular aging and environmental stress as compared to other αβ and γδ T cells.

2. Material and methods

2.1. Study design

2.1.1. Sample size

No power analysis was done. Sample size was based on sample availability.

2.1.2. Replicates

The experiments were repeated 3–5 times with similar composition of samples from the different groups at one point to minimize batch effect.

2.1.3. Randomization

We separate the samples from each group into different batches that have a similar number of samples from each group to minimize batch effect. The data processing was grouped.

2.1.4. Blinding

No blinding was done.

2.1.5. Ethnic statement

The study was conducted under National University of Singapore Institutional Review Board (IRB code NUS-IRB 01–256) and under NUS-IRB 10–250 for the apheresis cone.

2.2. Donor information

Participants of the study ($n = 22$, ≥60 years old) are enrolled in the Singapore Longitudinal Aging Study [16]. The young ($n = 24$, 21–40 years old) were recruited under National University of Singapore Institutional Review Board (IRB code NUS-IRB 01–256). Blood was collected in Cell Processing Tubes (CPT) (Becton Dickinson (BD)) and processed according to manufacturer's instructions. For characterization studies, blood from apheresis was obtained from Health Science Authority (HSA) Singapore, approved under NUS-IRB 10–250 and isolated using Ficoll-Paque (GE Healthcare).

Participants of the study for microbiome and peripheral blood immune composition association, ($n = 20$, >75 years old) is the same as mentioned previously (Table S1A-C).

2.3. Functional assay

PBMCs were suspended in either control medium (RPMI1640 supplemented with 10% FBS, and Penicillin (100 U/mL) Streptomycin (100 μg/mL) (Gibco)), with 1 μM of HMBPP; (Echelon Biosciences Incorporated) or with 10 ng/mL phorbol 12-myristate 13-acetate, (PMA; Sigma-Aldrich) together with 1 μM of calcium ionomycin (Sigma-Aldrich). Brefeldin A and Monesin (Thermo Scientific) was added in the last 4 h of stimulation. Stimulation was performed at 37 °C, 5% CO_2 for 6 h.

2.4. Proliferation assay

1 μg/mL of CD3 (OKT3, Thermo Scientific) was coated on a 96 well flat bottom plate in 37 °C, 5% CO_2 for 3 h and washed with PBS twice. CellTrace™ Violet (Invitrogen) was used to label the cells according to manufacturer's instructions. Labeled PBMCs were re-suspended in either 200μL of control medium, with recombinant 10 ng of IL-2 (R&D System) in CD3 plated wells or with 1 μM of HMBPP. PBMCs proliferated for 5 days in 37 °C, 5% CO_2.

2.5. Flow cytometry

PBMC were stained with antibodies as stated in Supplementary Table 2A for 20 min in the dark at 4 °C in PBS (5% FBS), 2 mM EDTA (FACS Buffer). For CD85j and CD244, cells were single stained with CD85j, followed by CD244 before adding the master mix to the cells (each staining is 20 min in the dark at 4 °C) (Fig. S1).

CD107a was added at the start of the stimulation. After stimulation, cells were stained with surface markers before being fixed and permeabilized for 20 min in 4 °C with BD CytoFix/CytoPerm Fixation and Permeabilization Solution (BD Biosciences). The cells were washed twice with 1× Perm/Wash Buffer (BD Biosciences). PBMCs were stained in 1× Perm/Wash with antibodies as stated in Table S2A for 30 min in 4 °C and washed twice before re-suspending in 100 μL FACS buffer.

Samples were acquired using BD LSRII/Fortessa/FACSSymphony flow cytometer using automatic compensations.

Please cite this article as: W. Xu, G. Monaco, E.H. Wong, et al., Mapping of γ/δ T cells reveals Vδ2+ T cells resistance to senescence, EBioMedicine, https://doi.org/10.1016/j.ebiom.2018.11.053

2.6. Flow-fish

Using the antibodies as stated in Table S2B, samples were then washed in PBS, fixed in 1 mM BS3 (30mins on ice, Thermo Scientific, USA) and quenched with 50 mM Tris in PBS (pH 7.2, 20 mins, RT). Cells were then washed twice; first in PBS, and then in hybridization buffer (70% deionized formamide, 28.5 mM Tris HCL pH 7, 1.4% BSA and 0.2 M NaCl). Subsequently the samples were re-suspended in hybridization buffer and incubated with 0.75 μg/mL of the PNA TelC-Cy5 probe (Panagene, South Korea) and heated for 10 min at 82 °C. Samples were then rapidly cooled on ice and left to hybridize for 1 h at RT in the dark. Lastly, samples were washed twice in post hybridization buffer (70% deionized formamide, 14.25 mM Tris HCL pH 7, 0.14% BSA, 0.2 M NaCl, 0.14% Tween20) and twice in 2% BSA/PBS before acquisition on BD Fortessa using BD FACS Diva software.

2.7. DNA damage repair (DDR) assay

PBMCs was re-suspended in control medium and were UV-irradiated for 6 h (6amp, UVC) using Gelman BH Class 2 Series biological safety cabinet with lid on 96 well U-bottom plate. Controls were placed in 37 °C, 5% CO2 for 6 h. PBMCs were stained with antibodies as stated in Table S2C for 20 min in 4 °C. PBMCs were washed twice. After washing, PBMCs were fixed using BD Cytofix Buffer at 37 °C for 10mins. After washing, 300ul of BD Phosflow Perm Buffer 2 was used to permeabilize the cells for 30mins at 4 °C. After permeabilization, anti-H2AX phospho (Ser139) were added for 30mins at RT in the dark. PBMCs were washed twice and re-suspended in 100 μL of FACS Buffer before acquisition.

2.8. CYTOF

2.8.1. Antibodies conjugation and CyTOF staining

Frozen samples were thawed using RPMI 10% FBS + DNase (15μg/mL). Cells were stained with Cisplatin and DNA as described [17] After wash, cells were stained in PBS + 0.5% BSA buffer with antibodies at 4 °C for 15mins. After washing twice, cells were fixed in fixation FoxP3 buffer (eBioscience) for 30 min at 4 °C. After washing in perm buffer, cells were stain with αEomes-PE for 30 min at 4 °C in perm buffer. Cells were washed and stained with intracellular markers for 30 min at 4 °C in perm buffer. After washing twice, cells were fixed in PBS 2% PFA overnight.

2.8.2. Antibody conjugation

Purified antibodies were conjugated as stated in Table S3. Antibody conjugation was performed according to Fluidigm Inc. protocol.

2.8.3. Data analysis and t-SNE

After CyTOF acquisition, which was performed as previously described, any zero values were randomized using a uniform distribution of values between zero and minus-one using an R script (as was the default operation of previous CyTOF software). Note also that all other integer values measured by the mass cytometer are randomized in a similar fashion by default. The signal of each parameter was then normalized based on the EQ beads (Fluidigm) as previously described [18]. Cells were manually de-barocoded using FlowJo (Tree Star Inc.). Samples were then used for tSNE analysis similar to that previously described [24] using custom R scripts based on the "flowCore" and "Rtsne" (using CRAN R packages that performs the Barnes-Hut implementation of t-SNE) In R, all data were transformed using the "logicleTransform" function ("flowCore" package) using parameters: w = 0.25, t = 16,409, m = 4.5, a = 0 to roughly match scaling historically used in FlowJo. For heatmap, Median intensity corresponds to a logical data scale using formula previously describe. The colors in the Heat Map represent the measured means intensity value of a given marker in a given cluster. A four colors scale is used with black–blue indicating low expression values, green–yellow indicating intermediately expressed markers, and red representing highly expressed markers.

2.8.4. DA-Cell™ Luminex

FACS-sorted populations were stimulated with PMA/Ionomycin (10 ng/mL) for 4 h at 37 °C. PBMCs were pellet down at 1500 rpm at 4 °C with supernatant harvested and analyzed using DA-Cell™ Luminex bead-based multiplex assays based on the molecule of interest. Customized Kits information is in Table S4.

Using DA-96, samples or standards were incubated with fluorescent-coded magnetic beads, which had been pre-coated with respective capture antibodies. After an overnight incubation at 4 °C with shaking, plates were washed twice with wash buffer. Biotinylated detection antibodies were incubated with the complex for 30 min (for R&D Systems' protocol) or 1 h (for Merck's protocol) and subsequently Streptavidin-PE was added and incubated for another 30 mins. Plates were washed twice again, and beads were re-suspended with sheath fluid in PCR plates before acquiring on the FLEXMAP® 3D (Luminex). Data acquisition was done using xPONENT® 4.0 (Luminex) acquisition software and data analysis was done using Bio-Plex Manager™ 6.1.1 (Bio-Rad). Standard curves were generated with a 5-PL (5-parameter logistic) algorithm. Lastly, a report was generated with values for both MFI and concentration data.

2.8.5. Nanostring

FACS-sorted populations were stimulated with PMA/Ionomycin (10 ng/mL) for 4 h at 37 °C. PBMCs were pellet down at 1500 rpm at 4 °C. 6249–10,000 cells in 5uL of RLT buffer (Qiagen) were hybridized with probes from the nCounter Human Inflammation v1 panel and 10,000 cells (except for 3 samples with ~5500–7700 cells) in 5uL of RLT buffer (Qiagen) were hybridized with probes from the nCounter Human Senescence custom panel at 65 °C for 19 h according to nCounter™ Gene Expression Assay Manual. The nCounter™ Digital Analyzer (GEN1) was used to quantify target molecules present in each sample. A high-density scan (600 fields of view) was performed.

2.8.6. CMV serology

Plasma from the participants were thawed and analyzed for the presence of CMV IgG antibodies according to the manufacturer's instructions (Omega Diagnostics).

2.8.7. Epigenetic methylation RRBS data and analysis

2.8.7.1. DNA preparation. Liquid nitrogen snap-frozen FACS-sorted cells samples were thawed and Pure Link Genomic DNA extraction kit (Invitrogen) was used as manufacturer's instructions and RRBS-seq was performed as described [19]. In brief, 50 ng of purified DNA was digested with *Msp*I (Fast digest MspI, Thermo Scientific FD0544, USA) for 30 min at 37 °C followed by heat inactivation at 65 °C for 5 mins. Library preparation was performed using NEBNext Ultra DNA library prep kit for Illumina (New England BioLabs, E7370L, USA) and ligated with methylated adapters for Illumina at a dilution of 1:10 (New England BioLabs, E7535L, USA). The adapter ligated DNA was subjected to bisulfite conversion with EpiTect fast bisulfite conversion kit (Qiagen, 59,824, Germany) using the following cycling conditions: 2 cycles of (95 °C; 5mins, 60 °C; 10mins, 95 °C; 5mins, 60 °C; 10mins) and hold at 20 °C. Bisulfite converted DNA was PCR amplified for 14–16 cycles using 2.5 U of Pfu Turbo Cx Hotstart DNA polymerase (Agilent Technologies, 600,410) and size selected for fragments between 200 bp to 500 bp with Ampure Xp magnetic beads (Agencourt, A63880, USA). The purified DNA was subjected to single end sequencing using the Illumina Hiseq 2000 at 1 × 101 bp readlength.

2.8.7.2. DNA methylation data processing. RRBS-seq reads were aligned to the human reference genome, hg19, using Bismark with default parameters. CpGs with Q < 30 and read depth of <5× were filtered

Please cite this article as: W. Xu, G. Monaco, E.H. Wong, et al., Mapping of γ/δ T cells reveals Vδ2+ T cells resistance to senescence, EBioMedicine, https://doi.org/10.1016/j.ebiom.2018.11.053

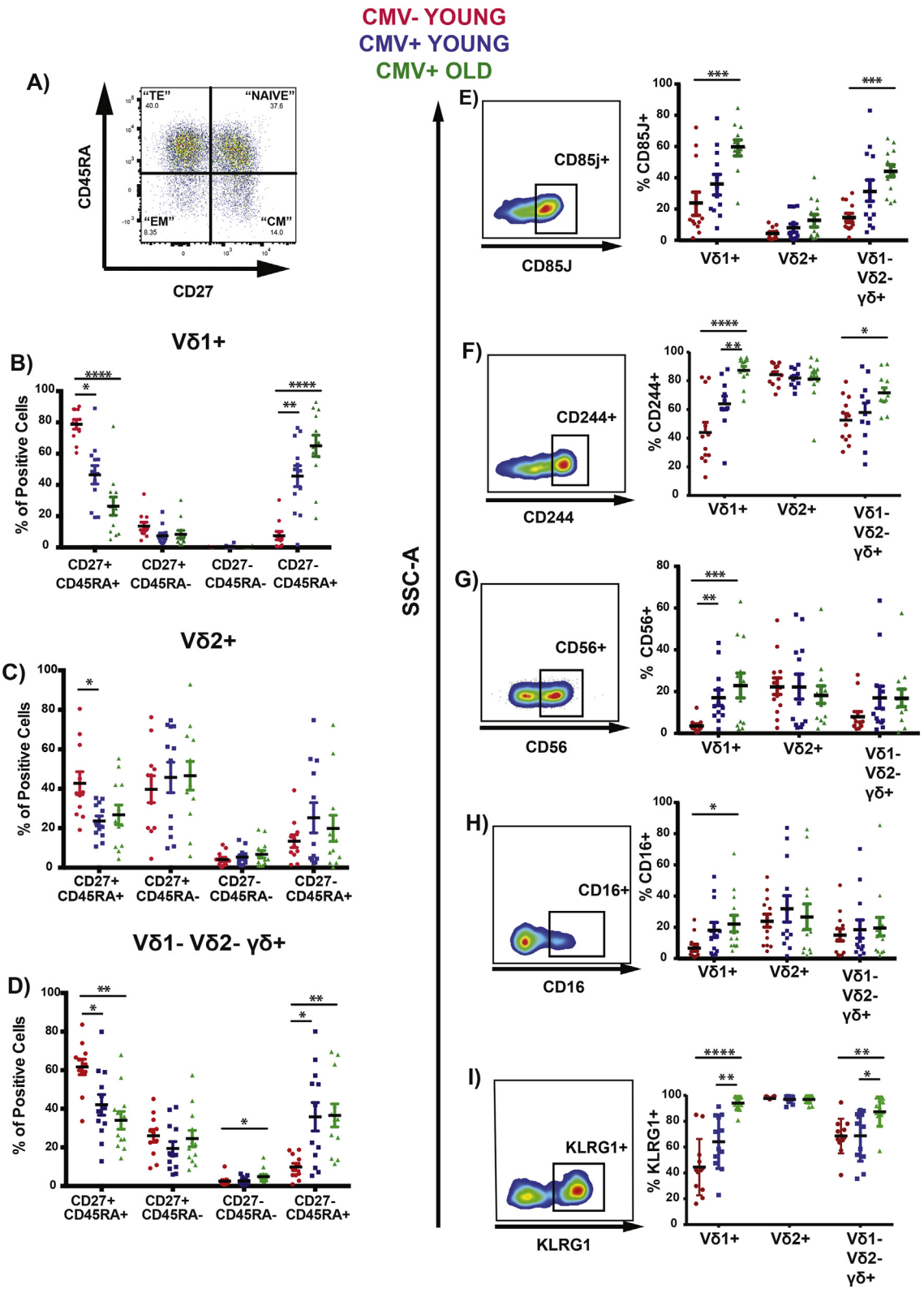

Fig. 1. Phenotypic Alterations of Vδ1+, Vδ2+ and Vδ1- Vδ2- γδ + in the young and elderly. CMV- Young (RED) $n = 12$, CMV+ Young (BLUE) n = 12, CMV+ Elderly (GREEN) n = 12 individuals PBMCs were stained and analyzed by flow cytometry. (A) Representative FACS plots of CD27, CD45RA. Frequency of the different subsets of CD27 and CD45RA for (B) Vδ1 +, (C) Vδ2+, (D) Vδ1- Vδ2- γδ + Representative FACS plot and Frequency of the γδ T cells for (E) CD85j+, (F) CD244+, (G) CD56+, (H) CD16+,(I) KLRG1+ (* = $p < 0.05$, ** = $p < 0.01$, *** = $p < 0.001$, **** = $p < 0.0001$). Kruskal-Walis Test and multiple *t*-tests (corrected with Dunn's Method) was performed. (For interpretation of the references to colour in this figure legend, the reader is referred to the web version of this article.)

out before calculating the percentage methylation (PM). PM is calculated for each covered C by taking the ratio of reads called methylated C divided by the total number of methylated and unmethylated reads. High read cutoff was applied to eliminate PCR effects. CpGs having higher coverage than 99.9% percentile of read counts were removed.

Please cite this article as: W. Xu, G. Monaco, E.H. Wong, et al., Mapping of γ/δ T cells reveals Vδ2+ T cells resistance to senescence, EBioMedicine, https://doi.org/10.1016/j.ebiom.2018.11.053

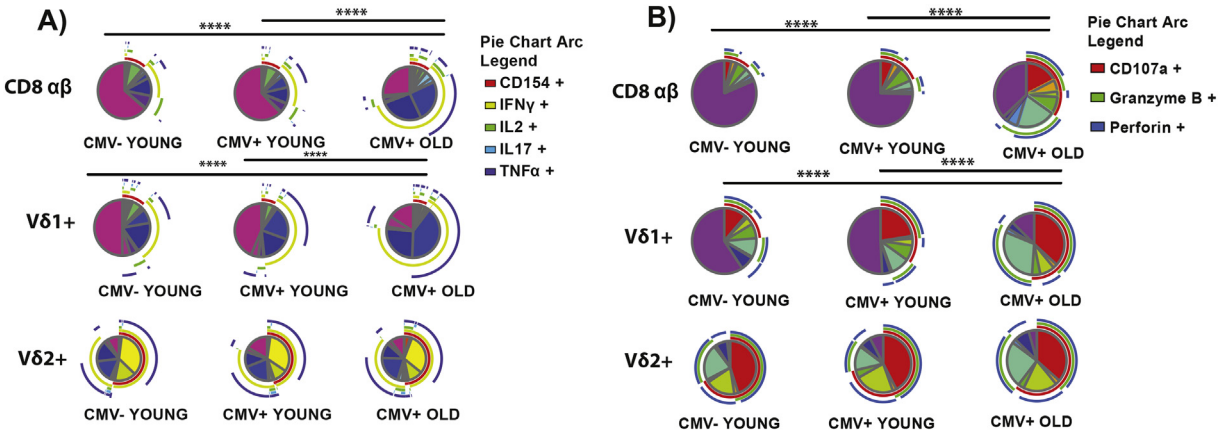

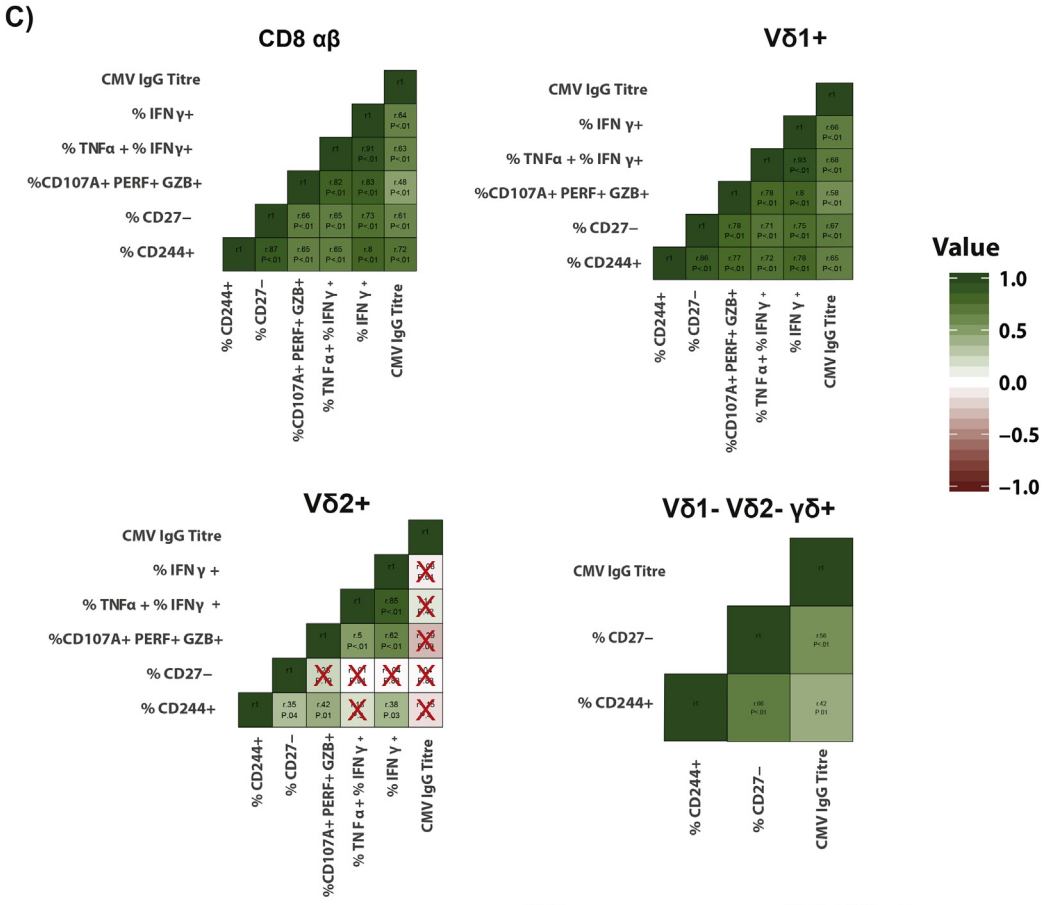

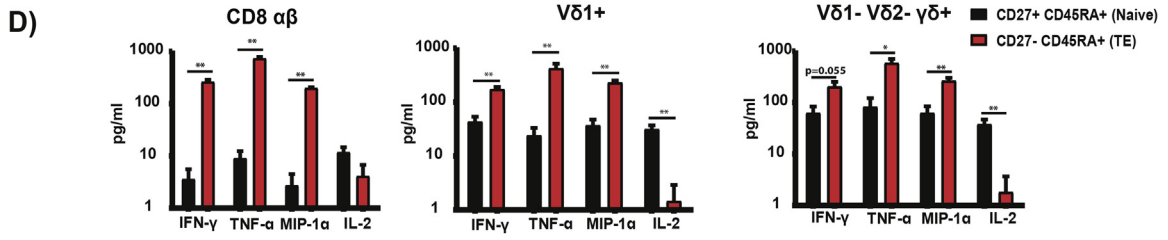

Please cite this article as: W. Xu, G. Monaco, E.H. Wong, et al., Mapping of γ/δ T cells reveals Vδ2+ T cells resistance to senescence, EBioMedicine, https://doi.org/10.1016/j.ebiom.2018.11.053

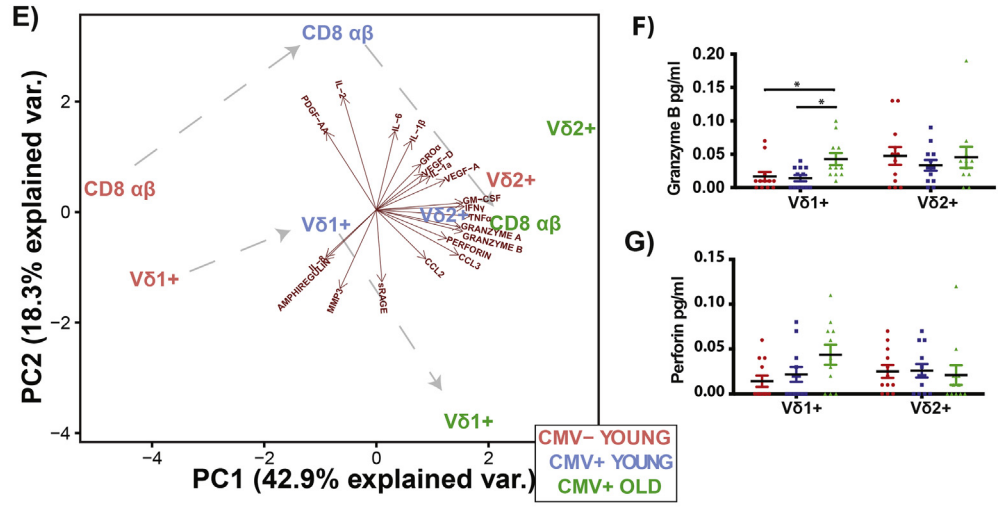

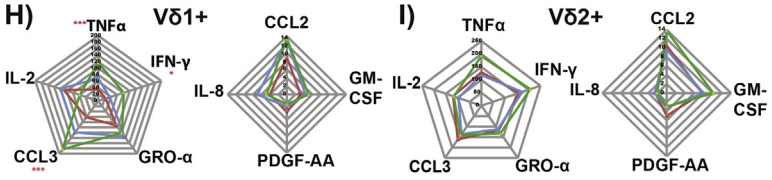

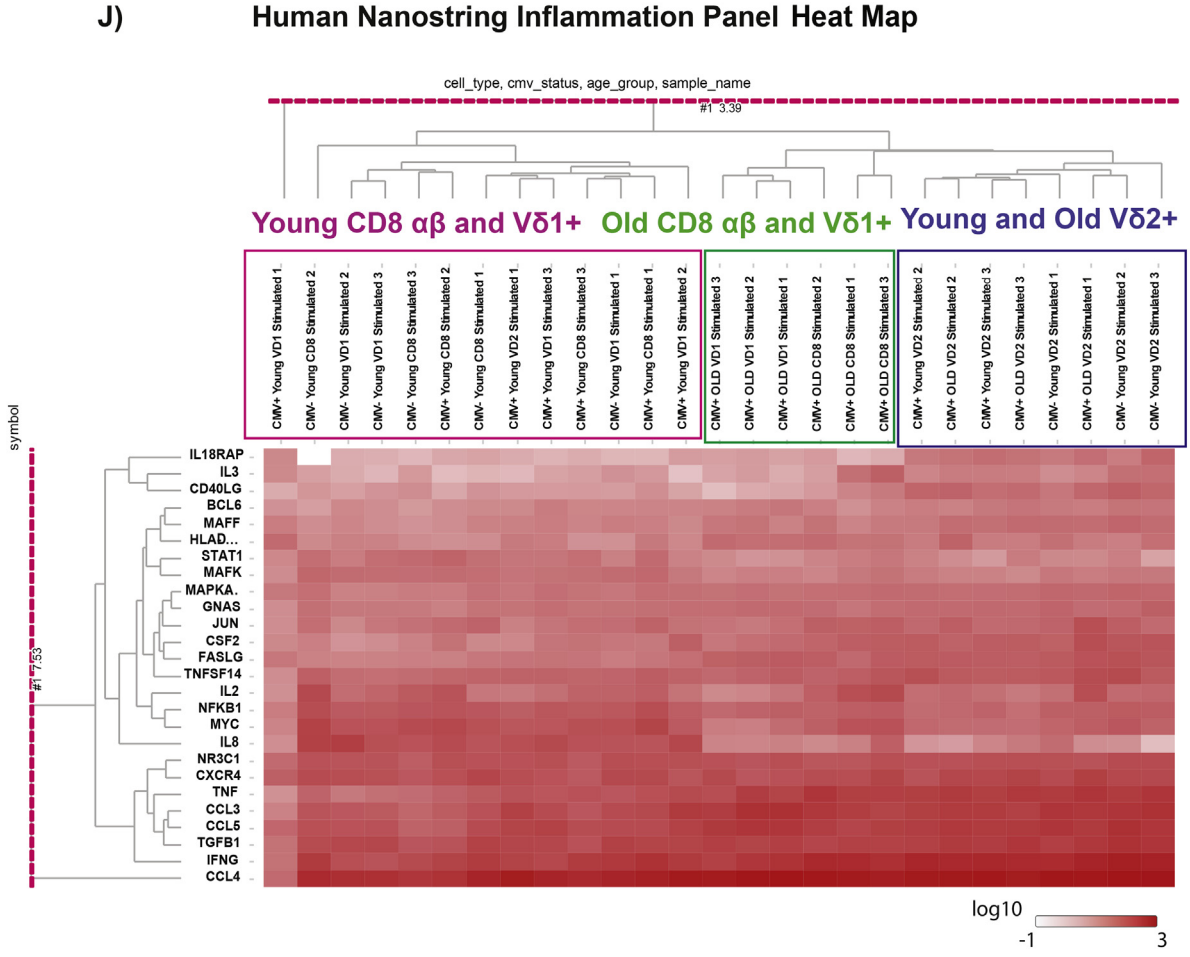

Please cite this article as: W. Xu, G. Monaco, E.H. Wong, et al., Mapping of γ/δ T cells reveals Vδ2+ T cells resistance to senescence, EBioMedicine, https://doi.org/10.1016/j.ebiom.2018.11.053

2.8.7.3. Differentially methylated CpGs analysis. DmCpG analysis was performed using R package Methylkit [20]. High coverage bases were filtered. Read coverages between samples were also normalized. Logistic regressions were used to calculate *P*-values for dmCpGs. P-values were adjusted to Q-values using SLIM method. After q-value calculation, differentially methylated regions were selected based on q-value and percent methylation difference cutoffs [q-value <0.01, meth.diff>20].

2.9. WGCNA

Beta values from significant dmCpGs were used to construct methylome modules using weight gene correlation network analysis (WGCNA) [thresholding power 6, minimum module size of 30, mergeCutHeight 0.15]. Eigengene for each module was correlated to the differentiation time point. Modules that showed significant association were visualized using heatmap and boxplots [absolute correlation coefficient, $r > 0.75$, p-value<.01].

2.10. RNA-Seq

2.10.1. RNA preparation

RNA was extracted using RNA isolation by TRIzol (Thermo Scientific) followed by Qiagen RNeasy Micro clean-up procedure (Qiagen). RNAs were analyzed on Agilent Bioanalyzer with RNA Integrity Number (RIN) range from 6.2 to 9.

2.10.2. RNA-Seq library preparation

cDNA libraries were prepared using 2 ng of total RNA and 1μL of a 1:50,000 dilution of ERCC RNA Spike in Controls (Ambion® Thermo Scientific) using SMARTSeq v2 protocol [21] with modifications listed in Table S5. Length distribution of the cDNA libraries was monitored using DNA High Sensitivity Reagent Kit on Perkin Elmer Labchip (Perkin Elmer). All samples were subjected to an indexed PE sequencing run of 2×51 cycles on an Illumina HiSeq 2000 (16 samples/lane).

2.10.3. RNA-Seq data analysis

The genome assembly and annotation for the RNA-Seq data analysis was downloaded from GENCODE (version 26) [22]. The quality of the RNA-Seq data was assessed with FastQC [23]. The reads were pseudo-aligned to the transcriptome with kallisto [24], and the transcript expression values were summarized into gene expression values with tximport [25]. The counts were normalized for sequencing depth and gene length using the Transcript per Million (TPM) method [26].

The RNA-Seq data is available as part of a larger GEO repository with accession number GSE107011.

2.11. GSEA

Averaged gene expression data in the form of log2 RPKM (reads per kilobase of transcript, per million mapped reads) values were used to rank the genes for each of the cell type. Ranked list was checked for enrichment in the Vδ2+ gene set using a Gene Set Enrichment Analysis (GSEA). GSEA was conducted using the fgsea package in bioconductor running using R version 3.3.1.

2.12. 16S microbiome sequencing

2.12.1. Sample preparation

Stools were collected and frozen in aliquots with glass beads. Stools were then resuspended in Breaking Buffer (2% (v/v) Triton X-100, 1% (v/v) SDS, 100 mM NaCl, 10 mM Tris-HCl(pH: 8.0), 0.1 mM EDTA (pH:8.0). After breaking down the stools, DNA was extracted using Phenol/Chloroform method with RNase A as shown in [27].

2.12.2. Preparation of 16S amplicon libraries

For amplification of the 16 s variable regions, PCR was performed using 10 ng of gDNA prepared from gut metagenome samples with Long Amp Taq polymerase (New England Biolabs, USA) as described in Jones et al. 2016 [28],. In brief, first round of PCR enriches for V4 & V5 regions of bacterial 16 s rDNA regions and incorporates partial Illumina adapter sequences. The secondary PCR further enriches for variable region sequences while adding complete Illumina adapter tags, barcodes for sequencing and demultiplexing individual samples, respectively. Equimolar concentrations of secondary PCR products were pooled and electrophoresed using 2% agarose gel. This pool of libraries was size selected (~550 bp) by gel purification using Qiaquick Gel Extraction Kit (Qiagen, Germany). Concentrations of gel-purified libraries were estimated using LabChip GX reagents according to the manufacturer's instructions (PerkinElmer, USA). qPCR was performed (Kapa Biosystems, USA) using the quantified libraries to ascertain the loading concentration. The libraries were sequenced using Illumina MiSeq to generate 250 bp paired end reads.

2.12.3. 16S sequencing analysis

The FASTQ files obtained by the Illumina sequencing by synthesis protocol, from the fragments' library from the 16S amplification, had the Illumina-specific forward and reverse primers removed using Cutadapt; paired-end reads were joined together with the aid of Flash software, and a sliding window quality filter was applied using Trimmomatic.

A Perl pipeline mainly based on QIIME (Quantitative Insights into Microbial Ecology), designed for the microbial community analysis of DNA sequencing data, was followed. The hypervariable regions in the 16S gene that were amplified, provide species-specific signature sequences that were compared with known sequences in a reference database via the QIIME OTU (Operational Taxonomic Unit, the microbes in the community) picking method against the Silva database version 123 at 99% of redundancy.

R and Spotfire were used respectively to read the QIIME resulting OUT table, calculate relative OTU percentage abundances at genus level and plot the values in stacked bar plots.

2.13. Data analysis and visualisation

For analysis of flow cytometric data, FlowJo version 10.06 was used. Statistical analysis was performed using Prism 6 (Graph Pad Software, Inc. La Jolla). For comparisons between two independent groups, the Mann-Whitney *U* Test was performed. For comparisons between 3 or more independent groups, Kruskal-Walis Test and multiple *t*-tests

Fig. 2. Functional Capacity of CD8 αβ, Vδ1+ and Vδ2+ in the young and elderly. CMV- Young ($n = 12$), CMV+ Young (n = 12) and Elderly (n = 12) individuals PBMCs were stimulated by 10 ng/mL PMA together with 1 μM of calcium ionomycin for 6 h at 37 °C, stained and analyzed by flow cytometry. (A) SPICE Pies of Cytokines for CD8 αβ, Vδ1+, Vδ2+. (B) SPICE Pies of Cytotoxicity for CD8, Vδ1+, Vδ2+. (C) Spearman Correlation Heatmap Analysis using different parameters of CD8 αβ, Vδ1+, Vδ2+ and Vδ1- Vδ2- γδ+. (D) Multiplex beads analysis ($n = 6$) of CD27- CD45RA+ and CD27+ CD45RA+ of CD8 αβ, Vδ1+ and Vδ1- Vδ2- γδ+. 5 × 10^3 sorted cells were stimulated with PMA/Ionomycin (10 ng/ml) for 4 h. Supernatant were collected for Multiplex analysis. (E) PCA analysis profiling of CD8 αβ, Vδ1+ and Vδ2+ in CMV- Young, CMV+ Young and CMV+ Old. Concentration of (F) Granzyme B and (G) Perforin. (H) Analytes for Vδ1+, (I) Analytes for Vδ2+. For the Radar Graphs, the significance of the comparison between two groups is reported if significant, where blue denotes comparison between CMV- Young and CMV+ Young, green denotes comparison between CMV+ Young and CMV+ Old, red denotes comparison between CMV- Young and CMV+ Old. (**J**) Gene expression analysis of Inflammation Panel from Nanostring. 10,000 (pooled from 4 donors) cells of CD8 αβ, Vδ1+ and Vδ2+ were stimulated with PMA/Ionomycin. Top 26 genes were selected from PC1 as shown in Heatmap. (* = p < 0.05, ** = p < 0.01). *** = p < 0.005), **** = p < 0.0001). Monte Carlo was performed for A and B. Mann-Whitney *U* Test was performed for D. Kruskal-Walis Test and multiple *t*-tests (corrected with Dunn's Method) was performed F, G, H I. P–values <0.05 were considered significant. (For interpretation of the references to colour in this figure legend, the reader is referred to the web version of this article.)

Please cite this article as: W. Xu, G. Monaco, E.H. Wong, et al., Mapping of γ/δ T cells reveals Vδ2+ T cells resistance to senescence, EBioMedicine, https://doi.org/10.1016/j.ebiom.2018.11.053

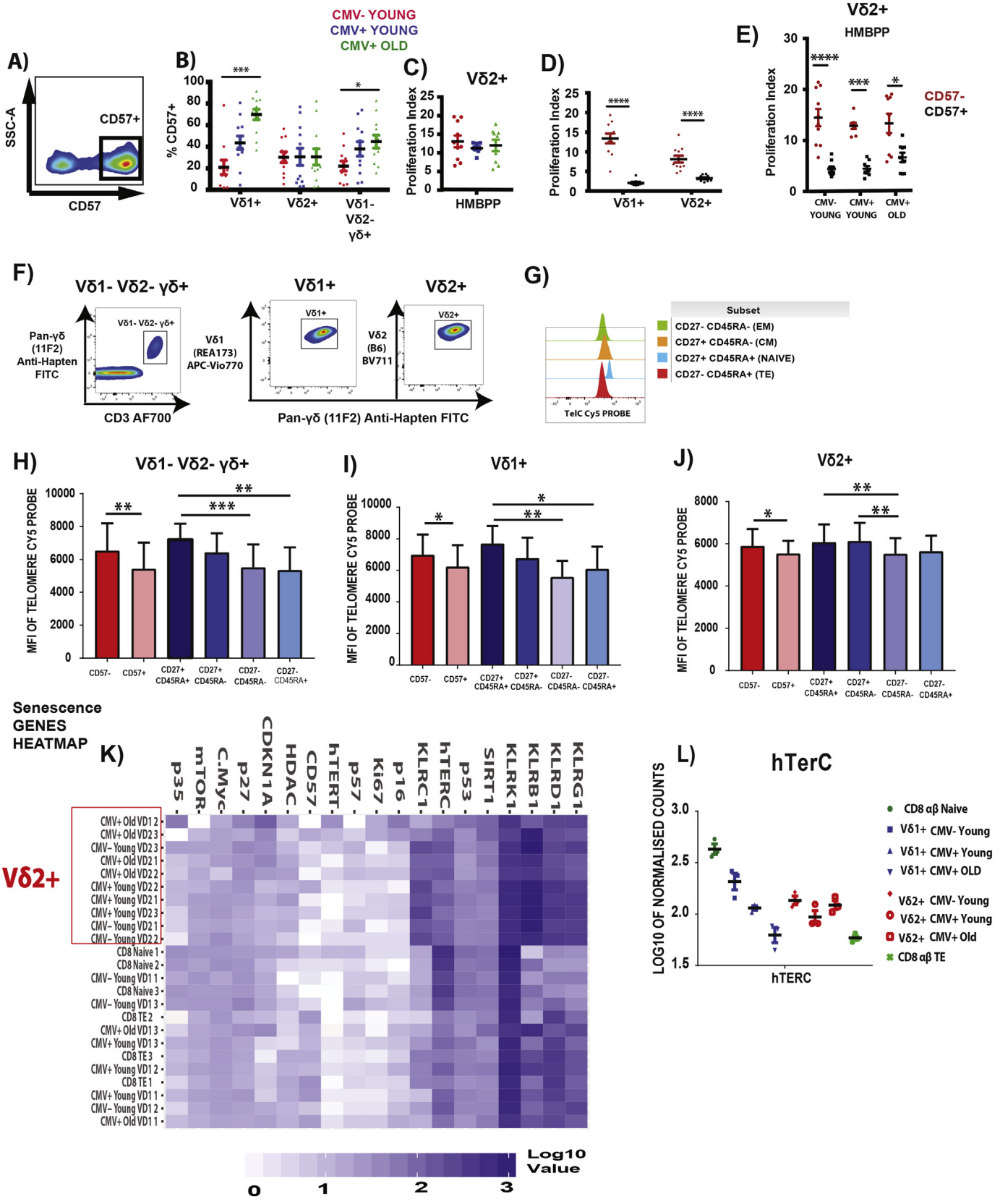

Please cite this article as: W. Xu, G. Monaco, E.H. Wong, et al., Mapping of γ/δ T cells reveals Vδ2+ T cells resistance to senescence, EBioMedicine, https://doi.org/10.1016/j.ebiom.2018.11.053

(corrected with Dunn's Method) was performed. For correlation analysis, spearman correlation was performed. For comparisons between paired samples with 3 or more groups, Friedman Test and multiple t-tests (corrected with Dunn's Method) was performed. *P* values <.05 (for 2 groups and correlation analysis) Adjusted P–values <0.05 were considered significant (for 3 or more groups).

SPICE version 5.1 and Monte Carlo was performed to compare between 2 SPICE pies in Fig. 2. Modfit LT version 3.2 was used to derive the proliferation index by floating method.

$$Proliferation\ Index = \frac{\sum_0^i N_i}{\sum_0^i N_i/2^i}$$

where I is the generation number (parent generation = 0).

In the absence of proliferation, that is, when all cells are in the parent generation, Eq. (1) gives:

$\frac{N_0}{N_0/2^0} = 1$, defining the lower limit of the PI.

GREAT Analysis [29] was used for Enrichment analysis of epigenetic genes in MeSalmon Module. RStudio v3.3.2, ggplot2 package and custom R scripts was utilized to obtain the correlation heatmap matrix, PCA, heatmap and module-trait relationship of epigenetic data. Cytoscape v3.5 was used to generate the association analysis in Supplementary Fig. 5.

3. Results

3.1. Phenotype of γδ T cells family in response to stress

Having defined a gating strategy and observed similar trends in terms of γδ T cells frequency with our small cohort as reported in other studies [30,31,32,33] (Fig. S1, 2A-2E), we investigated the phenotype of the γδ T cells subsets in relation with two contexts: CMV history and aging. We chose markers that were known to modulate in CD8 αβ T cells for reference as γδ T cells is able to exhibit cytotoxicity functions, similar to CD8 αβ T cells [34,35,36] (Supplementary Fig. 2F–K). In our analysis, we observed a decrease in frequency of Vδ1+ and Vδ1- Vδ2- γδ + (which are most likely Vδ3+ T cells) [37] "Naïve" (CD27+ CD45RA+) and an increase of "TE" (CD27- CD45RA+) for Vδ1+ and Vδ1- Vδ2- γδ + with CMV history and an additive effect of age for Vδ1 +. This trend was however not seen with Vδ2+ (Fig. 1B-1D). We then went on to assess the other phenotypic markers such as CD85j, CD244, CD56, CD16 and KLRG1. However, the expression was independent of CMV history and age for Vδ2+ contrarily to all other γδ T cells subsets populations (Fig. 1 E-I). Together, these results show that history to CMV and lifelong response to stresses affects the phenotype of the γδ T cells subsets differentially, with Vδ1+ and Vδ1- Vδ2- γδ + behaving very similarly to the adaptive CD8 αβ T cells.

3.2. Functions of γδ T cells family in response to stress

Moving on, we investigated the cytokine/cytotoxic capacity of γδ T cells subsets from the 3 groups. We stimulated the cells with PMA/Ionomycin and measured CD154, IFN-γ, TNF-α, IL-2, IL-17A, Granzyme B, Perforin and CD107a expression (surface). We observed that there was an increase in cells positive for these molecules with age but not CMV for CD8 αβ T cells and Vδ1+. However, Vδ2+ functional capacity was unaffected (Fig. 2A, B). We applied the same analysis for HMBPP-activated Vδ2+ but the results also showed no differences in functionality for Vδ2+ in the 3 groups. (Fig. S3A, B). These results showed that Vδ2+ functional capacity is sustained with aging.

We then correlated the different datasets (phenotype, CMV IgG titer and functional capacity) and found that Vδ1+ is similar to CD8 αβ T cells, as all the parameters showed positive correlation. However, this was not the case for Vδ2+, suggesting that the markers CD27/CD45RA do not functionally define Vδ2+ the same way as it is used to define CD8 αβ T cells (Fig. 2C). With this in mind, we FACS-sorted the two "extreme" stages (Naïve: CD27+ CD45RA+ and TE: CD27- CD45RA+) of CD8 αβ T cells, Vδ1+, Vδ1- Vδ2- γδ + and analyzed TNF-α, IFN-γ, MIP-α and IL-2 in response to PMA/Ionomycin stimulation. The data confirms that classification of γδ (other than Vδ2+) and αβ T cells is applicable and is similar using the same phenotypic markers (Fig.2D). This is further reinforced by our characterization of Vδ2+ and Vδ2- subsets using CYTOF and t-SNE analysis, where we included various surface markers, intracellular molecules, transcription factors and showed that the expression of CD27 separates Vδ2- into functionally distinct cluster but not Vδ2+. (Fig. S3C). With no clear differentiation path (phenotype/function) for Vδ2+ using these classical markers, we expanded our investigation to other molecules that have been associated with the Senescence Associated Secretory Profile that was established on fibroblasts (SASP) [38]. However, even though we used different methods and approaches, (Fig. 2E-I, Fig. S3D–F) the results converge to the same conclusion as previous results that Vδ2+ T cells do not exhibit a SASP profile with CMV history and age. This was further reinforced by gene expression analysis of inflammation-associated genes (Fig. 2J). Together, these results show that Vδ2+ do not behave as the rest of γδ T cells subsets in regard to differentiation and functional adaptation following challenges encountered during lifespan even though we included more targets in this study as compared to previous one [39].

3.3. CD57 expression and telomere length balance in Vδ2+

CD57 is a marker that implies replicative senescence when expressed on αβ T cells [40] (Fig. S4A–C) but the marker's functional implication has not been studied on γδ T cells subsets. We first compared the frequency of CD57+ γδ T cells subsets in the 3 groups and observed that the frequency increased with CMV and age for Vδ1+ and Vδ1- Vδ2- γδ + but not Vδ2+ (Fig. 3B). We then went on to investigate the proliferation capacity of Vδ2+ using HMBPP but we did not find any difference between the 3 groups (Fig. 3C). Moving on, we compared the proliferation capacity of CD57-, CD57+ of Vδ1+ and Vδ2+ using different stimulation. We observed that CD57- has a higher proliferation capacity compared to CD57+ for both Vδ1+ and Vδ2+. This difference is also observed with HMBPP stimulation for Vδ2+. (Fig. 3D, E). These data imply that CD57 could be a universal marker of replicative senescence for αβ and γδ T cells but the pool of replicative senescent Vδ2 + CD57+ T cells does not accumulate with CMV and age.

Another way to assess proliferative history and senescence is the erosion of telomeres. Surface marker expression using CD27/CD45RA

Fig. 3. Frequency and proliferation index of CD57+ γδ T cells in the young and elderly. CMV- Young (RED) (n = 12), CMV+ Young (BLUE) (n = 12) and Elderly (n = 12) (GREEN) individuals PBMCs were stained and analyzed by flow cytometry. (A) Representative FACS plots of CD57+. (B) Frequency of CD57+ of the γδ T cells subsets. (C) Proliferation Index of Vδ2+ in CMV- Young (RED), CMV+ Young (BLUE), CMV+ Old (Green) with HMBPP stimulation for 5 days. (D) Proliferation Index of Vδ1+ CD57- (RED) CD57+ (BLACK) and Vδ2+ CD57- (RED) CD57+ (BLACK) after CD3/IL-2 stimulation for 5 days (n = 12). (E) Proliferation Index of CD57- (RED) and CD57+ (BLACK) Vδ2+ in the respective group with HMBPP stimulation for 5 days. Telomere Length of CD27, CD45RA and CD57 subsets of γδ subsets. (F) Representative plots of the sorted populations after FLOW-FISH process. (G) Representation of histogram of the CD27/CD45RA subsets with TelC Cy5 Probe. Telomere Length of the various population and their CD27/CD45RA, CD57 subsets (*n* = 9) (H) Vδ1- Vδ2- γδ+, (I) Vδ1+, (J) Vδ2+. Vδ1+, Vδ2+ from CMV- Young (*n* = 3), CMV+ Young (n = 3), CMV+ Old (n = 3) and CD8 αβ Naïve, TE populations (CMV+ Young, n = 3) were used for the nanostring experiment (K) heatmap analysis of senescence-related genes are shown and (L) Normalized Count of hTerC gene expression (n = 3). (* = p < 0.05, ** = p < 0.01, *** = p < 0.001, **** = P < 0.0001). Kruskal-Walis Test and multiple *t*-tests (corrected with Dunn's Method) was performed for B, C. Mann-Whitney *U* Test was performed for D, E. Friedman Test and multiple t-tests (corrected with Dunn's Method) was performed for H. Adjusted P–values <0.05 were considered significant Adjusted P–values <0.05 were considered significant. (For interpretation of the references to colour in this figure legend, the reader is referred to the web version of this article.)

Please cite this article as: W. Xu, G. Monaco, E.H. Wong, et al., Mapping of γ/δ T cells reveals Vδ2+ T cells resistance to senescence, EBioMedicine, https://doi.org/10.1016/j.ebiom.2018.11.053

and CD57 are indicative of the telomere length in αβ T cells. However, whether these surface markers' expression is reflective of telomere length in the γδ T cells subsets remain uninvestigated. We quantified the length of the telomere in each subset for the different cell type using FLOW- Fluorescence in-situ hybridization (FLOW-FISH) that we modified from another study [41]. We observed that Vδ1+ and Vδ1- Vδ2- γδ + follows the trend of CD4 αβ T cells and CD8 αβ T cells with a decrease of telomere length from Naïve (CD27+ CD45RA+) to CM (CD27+ CD45RA-) and CM (CD27+ CD45RA-) to EM (CD27- CD45RA-). However, for Vδ2+ there is a decrease in telomere length but not in the same trend as the other cell types in the CD27/CD45RA subsets. In the case of the expression of CD57, CD57+ have a significant decrease in telomere length in all cell types including Vδ2+ when compared to CD57-, further reinforcing the functional relevance of CD57 to be universal in αβ and γδ T cells (Fig. 3H-J, Fig. S4D–I). To complement the above results, we assessed senescence-associated genes in the 3 different groups. We observed that the Vδ2+ clustered together independently of CMV status and age with senescence-related genes and also closer to the Naïve CD8 αβ T cells (Fig. 3K). We also observed that the RNA expression of hTerC, which controls the telomerase activity, is down regulated in the CMV+ Old when compared to CMV- Young in Vδ1+ but not Vδ2+ (Fig. 3L). Together, these results show that with CMV and age, Vδ2+ do not reach the stage of replicative senescence unlike the other γδ T cells subsets and αβ T cells.

3.4. RRBS Epigenetic Methylome Profile of CD4, CD8 and the γδ subsets

Biological age has been defined fairly precisely using the epigenetic clock developed by Steve Horvath [42]. We sought to test whether we could assess cellular aging by epigenetic screening to link with the above-mentioned Vδ2+ characteristics. Using the RRBS (Reduced Representation Bisulfite Sequencing) approach, we observed in general, a decrease in methylation as CD4 αβ T cells and CD8 αβ T cells differentiates from naïve to TE, which has been recently described even though they used a different approach for their epigenetic analysis [43,44] (Fig. S5A). We performed WGCNA to identify the gene modules that are highly significantly correlated with CD4 αβ T cells and CD8 αβ T cells differentiation stages. Using the genes in the MEBlue (increased methylation) and METurquoise (decreased methylation) gene modules, PCA was able to delineate CD4 αβ T cells and CD8 αβ T cells subsets as defined by flow cytometry (Fig. 4A). After establishing this, we input the data of the γδ subsets populations and observed that Vδ2+ remains clustered in the "CM" region, independently of their CD27/CD45RA profile (Fig. 4B) while the other cells show higher heterogeneity in the selected gene methylation profiles. We further investigated if there were possible epigenetic modifications unique to Vδ2+. Using a similar approach as above, we managed to identify a set of genes in the MESalmon module (Fig. S5C) that was hypo-methylated in Vδ2+. We employed enrichment analysis with this set of genes using GREAT and the (Fig. 4C) analysis revealed that the top significant pathway is the nicotinate and nicotinamide (NAD) metabolism pathway, which has been linked to cellular aging [45]. Collectively, these results show that Vδ2+ is unique on its own, while other γδ T cells subsets follow similarly to CD4 αβ T cells and CD8 αβ T cells, even on the epigenetic level.

3.5. Epi-transcriptomic analysis and DNA damage response capacity in Vδ2 +

Having identified a set of genes that are unique to Vδ2+ on the epigenetic level, we did a GSEA with the RNA-seq data set with the genes that were hypo-methylated in Vδ2+ to assess whether the epigenetic and transcriptomic level are aligned. We observed a significant enrichment of the genes only in Vδ2+, even though the donors of the 2 experiments were not the same. This suggests that these genes collectively are uniquely expressed at higher levels in Vδ2+ only (Fig. 5A). In the gene list, we identified a gene *MAD2L2*, that has been attributed with DNA repair at telomeres [46] and we found that there is higher level of expression in γδ T cells subsets compared to CD8 αβ T cells subsets (Fig. 5B). The ability of a cell to maintain and repair its genome is one of the hallmarks that prevent cellular aging [47]. Taking inspiration from this, we decided to investigate and assessed the DNA damage response (DDR) capacity of the γδ T cells subsets vs CD8 αβ T cells subsets by using p-H2AX (Ser139) as a marker of DDR capacity. Using 6 h of UV-irradiation to induce DNA damage, we observed a significant decrease in the expression of p-H2AX (Ser139) of CD8 αβ T cells and Vδ1+ in the differentiated CD27- population. However, this was not the case for Vδ2+ as its DDR capacity only decreased at the "TE" stage (CD27- CD45RA+) (Fig. 5E-H). This observation, together with previous phenotypic and functional observations, shows that Vδ2+ does not adhere closely to αβ T cells phenotypic classification.

4. Discussion

In this study, we thoroughly investigated the impact of aging and associated confounder (CMV infection) on the differential capacities of various γδ T cell populations towards differentiation and senescence. While much is known on γδ T cells, emerging data suggest a dichotomy between Vδ2+ and Vδ1+ T cells, especially regarding their belonging to the innate or adaptive arm of immunity.

We assessed the classical markers used to functionally define classical αβ T cells on the γδ T cells subsets, namely; CD27, CD45RA, CD57 and also other molecules. Besides the γδ T cell subsets phenotypic analysis, we coupled this investigation with the evaluation of their functional capacity such as cytokine/cytotoxic secretion, proliferation, telomere length, epigenetic profile and DNA damage response in relation to aging and its (CD27/CD45RA or CD57) phenotype.

The results showed that Vδ2- subsets (Vδ1+ and Vδ1- Vδ2- γδ+)but not Vδ2+ are adapting their phenotype and functional capacity similarly to CD8 αβ T cells, with CMV and age similar to another study [48]. The Vδ2+ adaptation to life-long stimulation is unique in terms of functional capacity, telomere length, epigenetic methylome profile and DNA damage response capacity.

The data in this study correlates well with two recent human γδ T cells studies. Ryan et al. showed that the phenotype of Vδ2+ is stable in each individual and not affected by age [49] while Davey et al. showed that the TCR repertoire of the "Naïve" (CD27+ CD45RA+) are more diverse compared to the "TE" (CD27- CD45RA+) for Vδ1+ but not Vδ2 + [50].

A recent twin study by Mangino et al. also showed that Vδ1+ immune traits are more influenced by the environment while Vδ2+ immune traits are more influenced by heritability [51]. Together with our datasets, it does suggest that Vδ1+ are more moldable ("adaptive-like") by stressors encountered during life while Vδ2+ are more resilient and have an "innate-like" behavior that perhaps is influenced by heritability.

Vδ2+ are unique lymphocytes as they do not reach the senescence stage with life-long stressors unlike other innate-like cells such as Vδ1 + and NK cells [52]. Possible explanations to why Vδ2+ are more resilient against cellular senescence could lie in their unique epigenetic and transcriptomic signatures. The genes that are hypo-methylated and highly transcribed are enriched in pathways mitigating cellular senescence such as NAD+ metabolism and biological oxidation as shown by the GREAT analysis. Maintenance of genomic material is another essential component in mitigating cellular senescence. We demonstrated that Vδ2+ DDR capacity is unlike Vδ1+ and CD8 αβ T cells, whereby the DDR capacity of Vδ1+ and CD8 αβ T cells decreases upon losing CD27 expression. Together with the higher expression of *MAD2L2* in γδ T cells, this suggest that the ability of the cell to have effector function capacity without compromising on its ability to maintain the integrity of its genomic material at both the core and telomere could be essential in preventing the cells from reaching the senescence stage with stressor as shown in Vδ2 + .

Please cite this article as: W. Xu, G. Monaco, E.H. Wong, et al., Mapping of γ/δ T cells reveals Vδ2+ T cells resistance to senescence, EBioMedicine, https://doi.org/10.1016/j.ebiom.2018.11.053

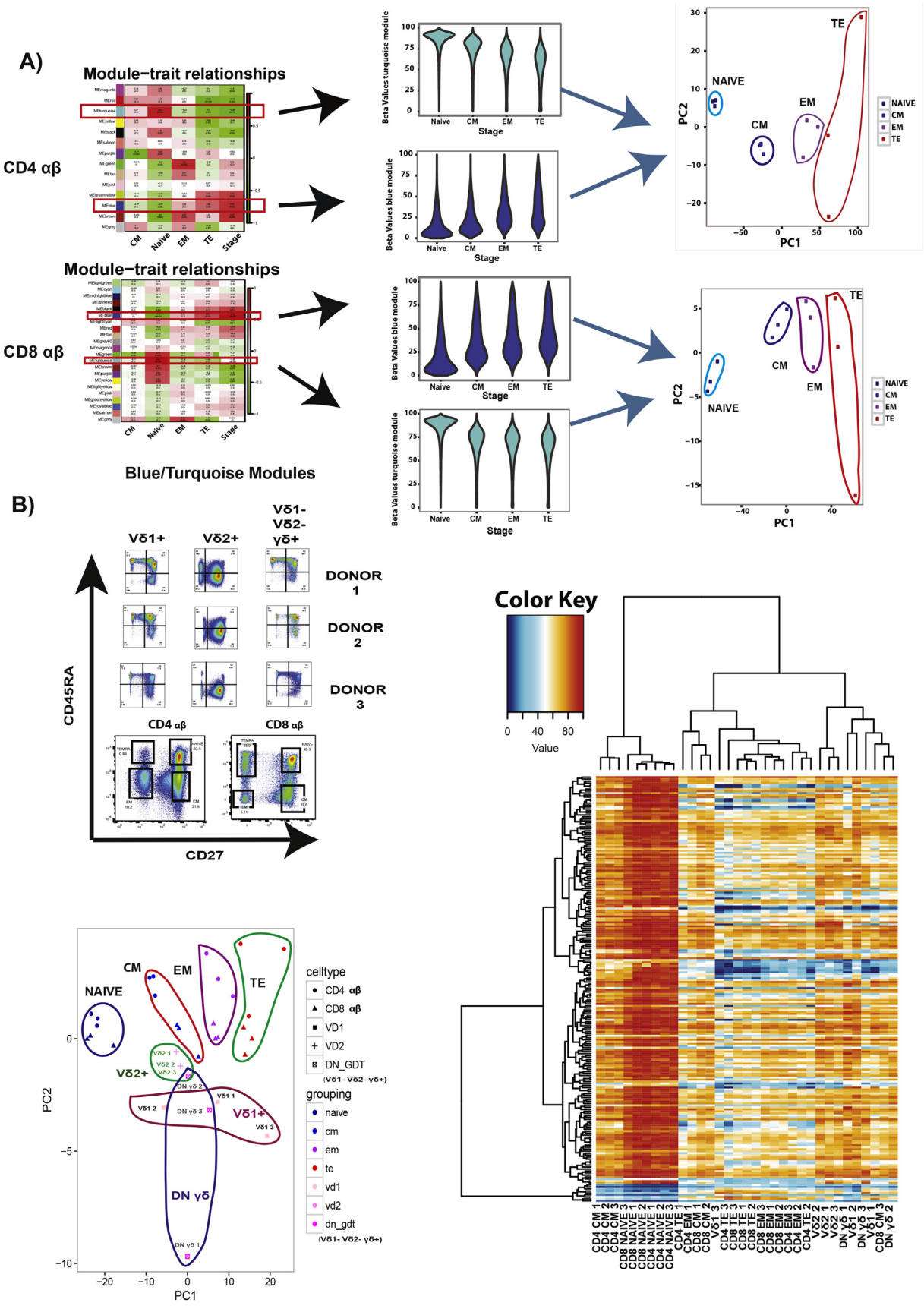

Please cite this article as: W. Xu, G. Monaco, E.H. Wong, et al., Mapping of γ/δ T cells reveals Vδ2+ T cells resistance to senescence, EBioMedicine, https://doi.org/10.1016/j.ebiom.2018.11.053

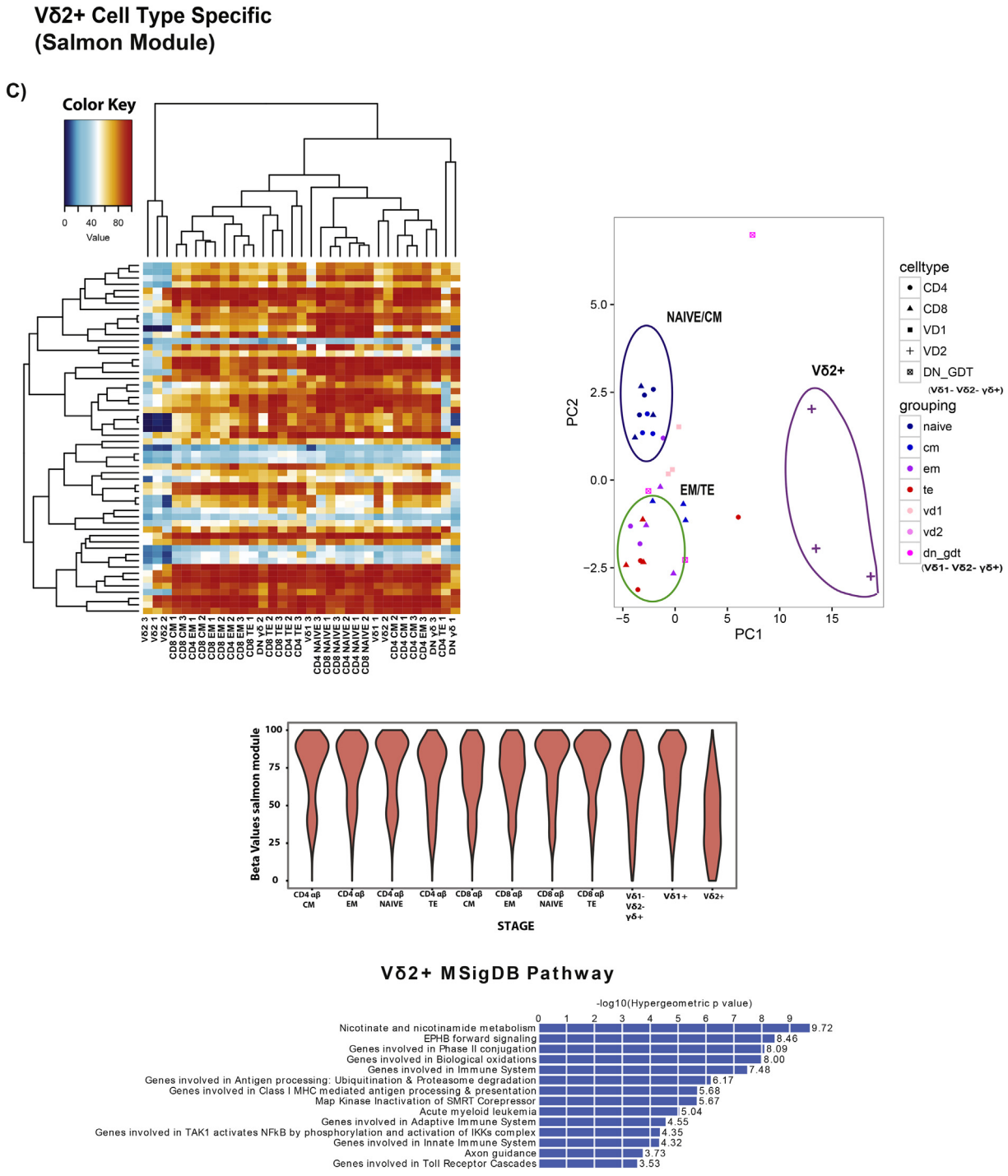

Fig. 4. Epigenetic profiles of CD4 αβ and CD8 αβ phenotypic subsets and the various γδ subsets. (A) Module Trait correlation matrix of the CD4 αβ and CD8 αβ differentiation stages. Beta values of gene methylation rate of genes in blue and turquoise modules in CD4 αβ and CD8 αβ. PCA analysis using genes from blue and turquoise module in CD4 and CD8 respectively. (B) Representative FACS plot of the phenotype of the individual γδ cell type from the different donors, and sorted CD4 αβ, CD8 αβ (Naïve, Memory Subsets). Heatmap clustering of genes from blue and turquoise modules from both CD4 αβ and CD8 αβ with the various γδ subsets. PCA analysis using genes of blue and turquoise module from CD4 αβ and CD8 αβ with the various γδ subsets. (C) Heatmap clustering of genes from MeSalmon module for the respective cell type. PCA analysis of genes from the MeSalmon module with the respective cell type, beta values of the genes from the MeSalmon module for the respective cell type. MSigDB Pathway Analysis using GREAT from genes of Salmon Module (FDR <0.05 and Enrichment set at 1.3-fold) (n = 3). (For interpretation of the references to colour in this figure legend, the reader is referred to the web version of this article.)

As for the biological relevance of surface marker expression, only CD57 have the same implication on both αβ T cells and Vδ2+ while most of them do not apply. This has also been shown with KLRG1 in another study [53] and could suggest that Vδ2+ might have a different ontogeny when compared to other γδ T cells subsets [54,55].

On a side note, the observed decrease of Vδ2+ in the elderly in the periphery is unlikely due to the well-known thymic involution [56] that occurs during lifespan as we did not observe a correlation between the frequency of Vδ2+ and CD4 RTE (a surrogate marker for thymic involution, CD4+ CD27+ CD45RA+ CD31+) (Fig. S5H). However, we did observe a correlation with the frequency of MAIT (Fig. S5J), suggesting that homeostasis of these 2 populations of T cells could be related. The other interesting finding is that the abundance of the bacteria *Parabacteriodes* in the gut correlates with the frequency of γδ/CD3 in

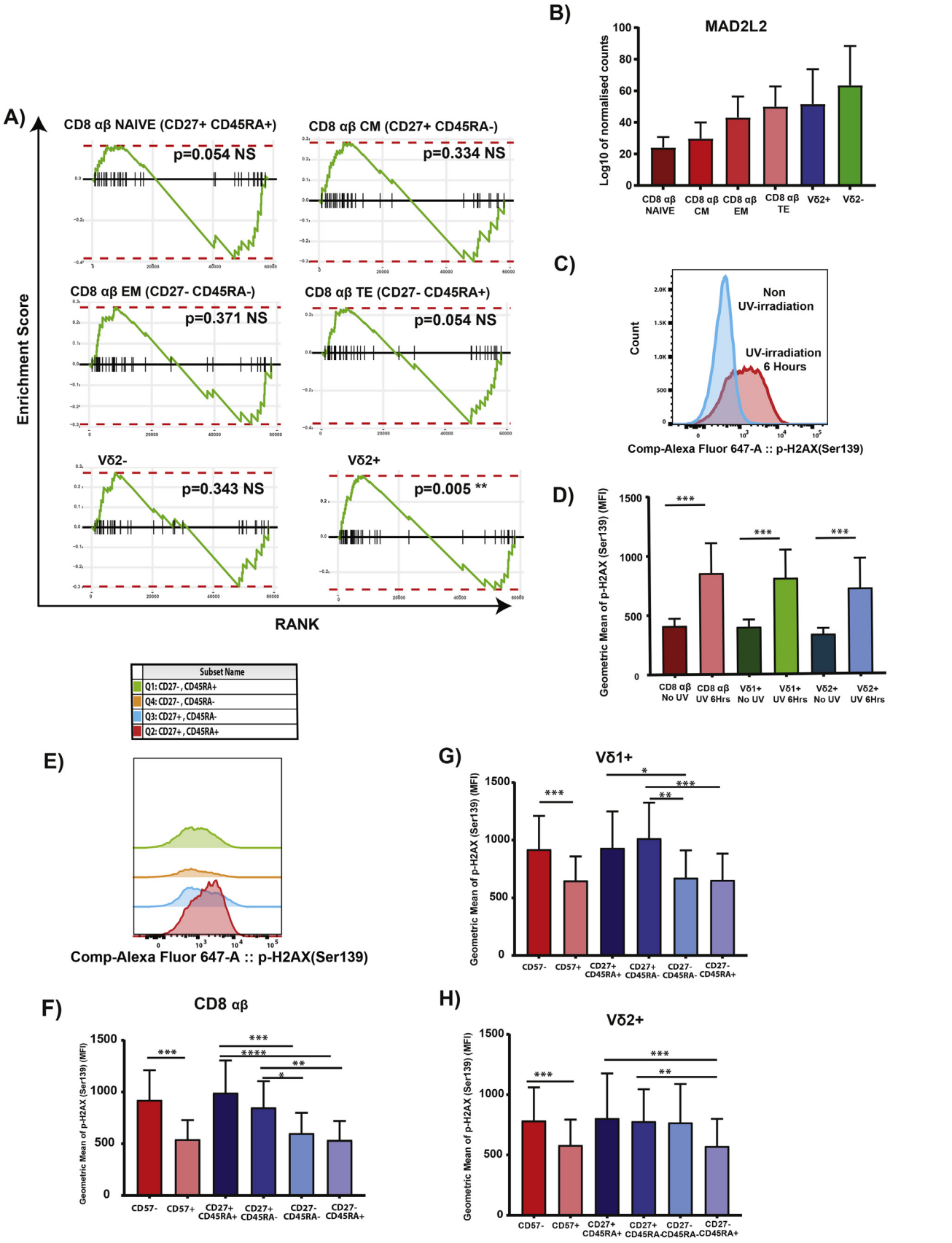

Fig. 5. DNA Damage repair response differs for Vδ2+ compared to CD8 αβ and Vδ1+ with differentiation. (A) GSEA analysis of genes in MeSalmon module with RNA-seq data. (B) Gene expression of *MAD2L2* in the different cell types. (C) Representative histogram of UV-induced expression of p-H2AX(Ser139). (D) Geometric MFI of p-H2AX with and without UV-induction. (E) Representative histogram of p-H2AX in the various subsets. Geometric MFI of p-H2AX of the subsets in (F) CD8 αβ, (G) Vδ1+ and (H) Vδ2+ . (* = $p < 0.05$, ** = $p < 0.01$, *** = $p < 0.001$, **** = $p < 0.0001$). Mann-Whitney U Test was performed for D. Friedman Test and multiple t-tests (corrected with Dunn's Method) was performed for F, G, and H. Adjusted P–values <0.05 were considered significant.

Please cite this article as: W. Xu, G. Monaco, E.H. Wong, et al., Mapping of γ/δ T cells reveals Vδ2+ T cells resistance to senescence, EBioMedicine, https://doi.org/10.1016/j.ebiom.2018.11.053

the periphery in the elderly, suggesting that the abundance of *Parabacteriodes* in the gut could explain the variation of γδ/CD3 frequency observed in the elderly (Fig. S5L, M) but overall has a minor importance in Vδ2+ homeostasis in aging.

It will also be important to investigate the γδ T cells subsets in the tissues, as the distributions of the γδ T cells subsets are different in each respective tissue. This will then give us insight on how their functions changes with age if any.

In conclusion, we showed that a strong dichotomy exists between the human γδ T cells subsets which follow different trajectories during aging. Most importantly Vδ2+ by their exceptional biological properties including epigenetics and DNA damage resistance are resistant to senescence. This is quite a unique model to exemplify the particular role of Vδ2+ in human biology. These findings also give credit to the notion that aging may be more of a differential adaption than a general immune alteration. Future work would enable to identify whether this potential of being resilient to stressors in Vδ2+ could be promoted in other cell type and consequently exploited to lead to better response to infections and in the field of cancer immunotherapy or designing a vaccine utilising Vδ2+ properties for the elderly.

Funding

Weili Xu is funded by A*STAR Graduate Academy (AGA). The work was funded by the Singapore Immunology Network, the Agency for Science Technology and Research (JCO grant #1434m00115) and the Skin Research Institute of Singapore (SRG grant #14018).

Author contributions

W.X. designed, performed the experiments, analyzed, interpreted the data, prepared the figures and wrote the paper. G.M. designed the RNA-seq experiments, analyzed the multiplex data and prepared the figs. E.W.H., W.L.W.T., R.F. provided the expertise, performed and analyzed the epigenetics data set. Y.S., H.K., S.W.T, E.N. provided the expertise, performed and analyzed the CYTOF data set. W.Z.Y·H wrote the custom R scripts and did the analysis of the senescence genes data set. C.T.Y.T. processed the human samples. S.K.G., D.C. provided the expertise, performed and analyzed the microbiome data set. I.C.H.L., E.W.H.M., S.F., J.L. performed the sorting, luminex and rna-seq/nanostring experiments respectively. B.T.K.L. analyzed the gene-array data. T.P.N. organized the elderly cohort and provided the blood samples. A.N.A. provided the expertise for FLOW-FISH experiments and intellectual directions. H.L.T, W.P.T and T.F provided background discussions. L.A. provided overall directions and wrote the paper; all authors have read and approved the final version of this manuscript.

Competing financial interests

Dr. Newell reports and cofounder, shareholder and on the board of directors of Immunoscape Pte. Ltd., an immune profiling service company. The other authors have no conflict of interests.

Acknowledgements

We would like to thank Ms. Christina Jia Ying Chu and the Functional Genomics Core Facility in SIgN for their expertise with the Nanostring and RNA-seq experiments, the FLOW Core Facility in SIgN for the sorting experiments, Dr. You Yi Hwang for proof-reading the manuscript and lastly, the healthy donors that have donated their blood for this study. We will also like to thank Agency of Science Technology and Research (A*STAR), A*STAR Graduate Academy (AGA), NHG-A*STAR-NTU for their funding in this study and also SIgN Immunomonitoring platform, supported by a BMRC IAF 311006 grant and BMRC transition funds #H16/99/b0/011.

Appendix A. Supplementary data

Supplementary data to this article can be found online at https://doi.org/10.1016/j.ebiom.2018.11.053.

References

[1] de Magalhães JP. How ageing processes influence cancer. Nat Rev Cancer 2013;13:357–65.
[2] Goldstein DR. Aging, imbalanced inflammation and viral infection. Virulence 2010;1:295–8.
[3] Goronzy JJ, Weyand CM. Understanding immunosenescence to improve responses to vaccines. Nat Immunol 2013;14:428–36.
[4] Vantourout P, Hayday A. Six-of-the-best: unique contributions of γδ T cells to immunology. Nat Rev Immunol 2013;13:88–100.
[5] Hayday A. C γδ cells: a right time and a right place for a conserved third way of protection. Annu Rev Immunol 2000;18:975–1026.
[6] Godfrey DI, Uldrich AP, Mccluskey J, Rossjohn J, Moody DB. The burgeoning family of unconventional T cells. Nat Rev Immunol 2015;11:1114–23.
[7] Bekiaris V, Sedy JR, Ware CF. Mixing Signals: Molecular turn Ons and turn Offs for Innate γδ T-Cells. Front Immunol 2014;5:1–7.
[8] Vermijlen D, Gatti D, Kouzeli A, Rus T, Eberl M. γδ T cell responses: How many ligands will it take till we know. Semin Cell Develop Biol 2018;84:75–86.
[9] Hayday AC. γδ T cells and the lymphoid stress-surveillance response. Immunity 2009;31:184–96.
[10] Groh V, Steinle A, Bauer S, Spies T. Recognition of stress-induced MHC molecules by intestinal epithelial γδ cells. Science 1998;279:1737–40.
[11] Gober HJ, Kistowska M, Angman L, Jeno P, Mori L, De Libero G. Human T cell receptor gammadelta cells recognize endogenous mevalonate metabolites in tumor cells. J Exp Med 2003;197:163–8.
[12] Puan KJ, Jin C, Wang H, et al. Preferential recognition of a microbial metabolite by human V γ 2Vδ2 T cells. Int Immunol 2007;19:657–73.
[13] Kared H, Camous X, Larbi A. T cells and their cytokines in persistent stimulation of the immune system. Curr Opin Immunol 2014;29:79–85.
[14] Larbi A, Fulop T. From 'truly naïve' to 'exhausted senescent' T cells: when markers predict functionality. Cytom Part A 2014;85:25–35.
[15] Xu W, Larbi A. Markers of T Cell Senescence in Humans. Int J Mol Sci 2017;18:1742.
[16] Ng TP, Feng L, Nyunt MSZ, Larbi A, Yap KB. Frailty in older persons: multisystem risk factors and the frailty risk index (FRI). J Am Med Dir Assoc 2014;15:635–42.
[17] Simoni Y, Fehlings M, Kløverpris HN, et al. Human Innate Lymphoid Cell Subsets Possess Tissue-Type based Heterogeneity in Phenotype and Frequency. Immunity 2017;46(1):148–61.
[18] Finck R, Simonds EF, Jager A, et al. Normalization of mass cytometry data with bead standards. Cytometry A 2013;83(5):483–94.
[19] Gu H, Smith ZD, Bock C, Boyle P, Gnirke A, Meissner A. Preparation of reduced representation bisulfite sequencing libraries for genome-scale DNA methylation profiling. Nat Protoc 2011;6:468–81.
[20] Akalin A, Kormaksson M, Li S, et al. methylKit: a comprehensive R package for the analysis of genome-wide DNA methylation profiles. Genome Biol 2012;13:R87.
[21] Picelli S, Faridani OR, Björklund AK, Winberg G, Sagasser S, Sandberg R. Full-length RNA-seq from single cells using Smart-seq2. Nat Protoc 2014;**9**(1):171–81.
[22] Harrow J, Frankish A, Gonzalez JM, et al. GENCODE: the reference human genome annotation for the ENCODE project. Genome Res 2012;22:1769074.
[23] Andrews S. FastQC: A quality control tool for high throughput sequence data. Available online at http://www.bioinformatics.babraham.ac.uk/projects/fastqc; 2010.
[24] Bray NL, Pimentel H, Melsted P, Pachter L. Near-optimal probabilistic RNA-seq quantification. Nat Biotechnol 2016;34(5):525–7.
[25] Soneson C. Love M.I., Robinson M.D.. Differential analyses for RNA-seq: transcript-level estimates improve gene-level inferences. F1000Res 2016;4:1521.
[26] Li B, Ruotti V, Stewart RM, Thomson JA, Dewey CN. RNA-Seq- gene expression estimation with read mapping uncertainty. Bioinformatics 2010;26(4):493–500.
[27] Pavelka N, Rancati G, Zhu J, et al. Aneuploidy confers quantitative proteome changes and phenotypic variation in budding yeast. Nature 2010;468(7321):321–5.
[28] Jones L, Ho WQ, Ying S, et al. A subpopulation of high IL-21-producing CD4 (+) T cells in Peyer's Patches is induced by the microbiota and regulates germinal centers. Sci Rep 2016 Aug **8**;6:30784.
[29] Cory YM, Dave B, Michael H, et al. GREAT improves functional interpretation of cis-regulatory regions. Nat Biotechnol 2010;28(5):495–501.
[30] Wistuba-Hamprecht K, Pawelec G, Derhovanessia E. OMIP-020: Phenotypic characterization of human γδ T-cells by multicolor flow cytometry. Cytom Part A 2014;85:522–4.
[31] Moncunill G, Han H, Dobani C, Juliana McElrath M. OMIP-24: Pan-leukocuyte immunophenotypic characterization of PBMC subsets in human samples. Cytom Part A 2014;85:995–8.
[32] Wistuba-Hamprecht K, Haehnel K, Janssen N, Demuth I, Pawelec G. Peripheral blood T-cell signatures from high-resolution immune phenotyping of γδ and αβ T-cells in younger and older subjects in the Berlin Aging Study II. Immun Ageing 2015;12.
[33] Roux A, Mourin G, Larsen M, et al. Differential Impact of Age and Cytomegalovirus Infection on the γδ T Cell Compartment. J Immunol 2013;191:1300–6.
[34] Tarazona R, Delarosa O, Alonso C, et al. Increased expression of NK cell markers on T lymphocytes in aging and chronic activation of the immune system reflects the accumulation of effector/senescent T cells. Mech Ageing Dev 2001;121:77–88.
[35] Pita-Lopez ML, Gayoso I, Delarosa O, et al. Effect of ageing on CMV-specific CD8 T cells from CMV seropositive healthy donors. Immun Ageing 2009;6:11.

Please cite this article as: W. Xu, G. Monaco, E.H. Wong, et al., Mapping of γ/δ T cells reveals Vδ2+ T cells resistance to senescence, EBioMedicine, https://doi.org/10.1016/j.ebiom.2018.11.053

[36] Henson SM, Akbar AN. KLRG1-more than a marker for T cell senescence. Age (Omaha) 2009;31:285–91.
[37] Vermijlen D, Brouwer M, Donner C, et al. Human cytomegalovirus elicits fetal γδ T cell responses in utero. J Exp Med 2010;207(4):807–21.
[38] Tan CYT, Witsuba-Hamprecht K, Xu W, et al. Vδ2 + and α / ß T cells show divergent trajectories during human aging. Oncotarget (Gerotarget) 2016;7:44906–18.
[39] Focosi D, Bestagno M, Burrone O, Petrini M. CD57+ T lymphocytes and functional immune deficiency. J Leukoc Biol 2010;87:107–16.
[40] Riddell NE, Griffiths SJ, Rivino L, et al. Multifunctional cytomegalovirus (CMV)-specific CD8+ T cells are not restricted by telomere-related senescence in young or old adults. Immunology 2015;144:549–60.
[41] Horvath S. DNA methylation age of human tissues and cell types. Genome Biol 2013; 14(10):R115.
[42] Durek P, Nordström K, Gasparoni G, et al. Epigenomic profiling of human CD4+ T cells supports a linear differentiation model and highlights molecular regulators of memory development. Immunity 2016;45(5):1148–61.
[43] Moskowitz DM, Zhang DW, Hu B, et al. Epigenomics of human CD8 T cell differentiation and aging. Sci Immunol 2017;2(8):eaag0192.
[44] Boersma V, Moatti N, Segura-Bayona S, et al. MAD2L2 controls DNA repair at telomeres and DNA breaks by inhibiting 5′ end resection. Nat Lett 2015;521: 537–40.
[45] Lopez-Otin C, Biasco MA, Patridge L, Serrano M, Koremer G. The hallmarks of aging. Cell Rev 2013;153(6):1194–217.
[46] Khairallah C, Dechanet-Merville J, Capone M. γδ T Cell-Mediated Immunity to Cytomegalovirus Infection. Front Immunol 2017;8:105.
[47] Ryan PL, Sumaria N, Holland CJ, et al. Heterogeneous yet stable Vδ2 (+) T-cell profiles define distinct cytotoxic effector potentials in healthy human individuals. PNAS 2016;113(50):14378–83.
[48] Davey MS, Willcox CR, Joyce SP, et al. Clonal selection in the human Vδ1 T cell repertoire indicates γδ TCR-dependent adaptive immune surveillance. Nat Commun 2017;8:14760.
[49] Mangino M, Roederer MR, Beddall MH, Nestle FO, Spector TD. Innate and adaptive immune traits are differentially affected by genetic and environmental factors. Nat Commun 2017;8:13850.
[50] Kared H, Martelli S, Tan SW, et al. Adaptive NKG2C+ CD57+ Natural Killer Cell and Tim-3 Expression during Viral Infections. Front Immunol 2018;9:686.
[51] Eberl M, Engel R, Aberie S, Fisch P, Jomaa H, Pircher H. Human Vγ9 / Vδ2 effector memory T cells express the killer cell lectin-like receptor G1 (KLRG1), 77; 2005; 16–9.
[52] De Rosa SC, Andrus JP, Perfetto SP, et al. Ontogeny of T cells in humans. J Immunol 2004;172:1637–45.
[53] Dimova T, Brouwer M, Gosselin F, et al. Effector Vγ9Vδ2 T cells dominate the human γδ fetal T-cell repertoire. PNAS 2015;112(6):E556–65.
[54] Junge S, Kloeckener-Gruissem B, Zufferey R, et al. Correlation between recent thymic emigrants and CD31+ (PECAM-1) CD4+ T cells in normal individuals during aging and in lymphopenic children. Eur J Immunol 2007;37:3270–80.
[55] Coppé J-P, Desprez PY, Krtolica A, Campisi J. The senescence-associated secretory phenotype: The dark side of tumor suppression. Annu Rev Pathol Mech Dis 2010; 5:99–118.
[56] Eric V. NAD+ in aging, metabolism, and neurodegeneration. Science 2015;350 (6265):1208–13.

Please cite this article as: W. Xu, G. Monaco, E.H. Wong, et al., Mapping of γ/δ T cells reveals Vδ2+ T cells resistance to senescence, EBioMedicine, https://doi.org/10.1016/j.ebiom.2018.11.053